Cyclosporine-loaded micelles for ocular delivery: investigating the penetration mechanisms

Martina Ghezzi[1], Ilaria Ferraboschi[2], Andrea Delledonne[2], Silvia Pescina[1], Cristina Padula[1], Patrizia Santi[1], Cristina Sissa[2], Francesca Terenziani[2], Sara Nicoli[1]*

[1] ADDRes Lab, Department of Food and Drug, University of Parma, Parco Area delle Scienze 27/A, 43124 Parma, Italy

[2] Department of Chemistry, Life Science and Environmental Sustainability, University of Parma, Parco Area delle Scienze 17/A, 43124 Parma, Italy

*Corresponding Author:

Sara Nicoli PhD
ADDRes Lab (Advanced Drug Delivery Research Lab)
Department of Food and Drug
University of Parma
Parco Area delle Scienze, 27/A
43124 Parma, Italy
Telefono +39 0521 905065/71
Fax +39 0521 905006
E-mail: sara.nicoli@unipr.it

Submitted to: Journal of Controlled Release

Abstract:

Cyclosporine is an immunomodulatory drug commonly used for the treatment of mild-to-severe dry eye syndrome as well as intermediate and posterior segment diseases as uveitis. The ocular administration is however hampered by its relatively high molecular weight and poor permeability across biological barriers. The aim of this work was to identify a micellar formulation with the ability to solubilize a considerable amount of cyclosporine and promote its transport across ocular barriers. Non-ionic amphiphilic polymers used for micelles preparation were tocopherol polyethylene glycol 1000 succinate (TPGS) and Solutol® HS15. Furthermore, the addition of alpha-linolenic acid was assessed. A second aim was to evaluate micelles fate in the ocular tissues (cornea and sclera) to shed light on penetration mechanisms. This was possible by extracting and quantifying both drug and polymer in the tissues, by studying TPGS hydrolysis in a bio-relevant environment and by following micelles penetration with two-photon microscopy. Furthermore, TPGS role as permeation enhancer on the cornea, with possible irreversible modifications of tissue permeability, was analyzed. Results showed that TPGS micelles (approx. 13 nm in size), loaded with 5 mg/ml of cyclosporine, promoted drug retention in both the cornea and the sclera. Data demonstrated that micelles behavior strictly depends on the tissue: micelles disruption occurs in contact with the cornea, while intact micelles diffuse in the interfibrillar pores of the sclera and form a reservoir that can sustain over time drug delivery to the deeper tissues. Finally, cornea quickly restore the barrier

properties after TPGS removal from the tissue, demonstrating its potential good tolerability for ocular application.

Keywords: cyclosporine, polymeric micelles, corneal delivery, transscleral delivery, TPGS hydrolysis, two-photon microscopy

Highlights

- TPGS micelles improved cyclosporine solubility promoting its retention in eye tissues
- Micelles disassemble in contact with the cornea
- Micelles diffuse intact inside the scleral tissue
- TPGS is hydrolyzed by tissue esterases when in contact with cornea and sclera
- Two-photon microscopy is a useful tool to study micelles-tissues interaction

1. Introduction

Cyclosporine A (CYC), a neutral cyclic peptide isolated from different fungal species, is an immunomodulatory drug which works inhibiting T cells activation by blocking the transcription of cytokine genes including those encoding for IL-2 and IL-4 [1]. Its main ocular application is the treatment of mild-to-severe dry eye syndrome (DES) and, with this indication, it is present as anionic O/W emulsion on the US market (0.05%, Restasis®) and as a cationic O/W nanoemulsion (0.1%, Ikervis®) on EU market. Moreover, an ophthalmic solution (0.09%, Cequa®) has been recently approved by the Food and Drug Administration. Together with the treatment of DES and other corneal affections [2, 3], cyclosporine has demonstrated its activity for the treatment of blepharitis [4, 5] as well as intermediate and posterior segment diseases including uveitis [6, 7] and Behçet disease [8].

The formulation of this drug and its delivery to ocular tissues are however hampered by its relatively high molecular weight (1202.6 g/mol), poor water solubility [9] and marked lipophilicity (log P= 3 [10]). Therefore, cyclosporine A is mainly administered via oily and surfactant-containing formulations [11], presenting low tolerability and side effects, such as ocular burning, vision interference, eye irritation and conjunctival hyperaemia [9, 12]. Moreover, cyclosporine higher affinity for the oily phase rather than the aqueous environment usually results in a poor bioavailability [12]. A possible alternative to solve these issues is represented by the use of micelles, i.e. colloidal systems formed by self-assembling of amphiphilic molecules ~~polymers~~ in solution at a concentration above the Critical Micellar Concentration (CMC). Surfactant micelles, made by low molecular weight compounds, show high CMC and thus low physical stability. On the contrary, polymeric micelles, i.e. micelles formed by amphiphilic polymers, are characterized by lower CMC and better stability against dilution, and are generally preferred as drug delivery systems. Micelles are composed of an inner lipophilic core, involved in drug loading and release, and an external hydrophilic shell, responsible for micelles interaction with body targets. These nanosystems, in addition to a relatively easy preparation, sterilization method and high scale-up feasibility, showed good solubilization properties and efficient cellular internalization [13-15]. In case of ocular delivery, micelles have demonstrated the ability to enhance drug transport to the anterior eye segment [16-18] thanks to an improved solubility of drugs, higher penetration capacity (due to their nanometric size) and prolonged drug release [19-21]. Furthermore, ex-vivo data highlighted their capability to promote drug permeation across ocular tissues such as the sclera and the choroid, in the perspective of a posterior segment targeting [16, 21, 22]. It is also worth mentioning that an extremely recent review identifies the word “micelles” as one of latest high-frequency keywords, including this vehicle among the emerging frontiers in ocular drug delivery [23]. Unfortunately, the intense academic research has not necessarily been followed by actual industrial development. The reasons are different, related to stability problems and difficulty of characterization [13, 24], but also to the scarce information available regarding the fate of the polymer following ocular administration. This aspect should be investigated since it provides numerous information: first of all, the quantification of the polymer in the various tissues allows us to elucidate the transport mechanisms, a non-trivial action in the case of micelles that, being association colloids, can undergo considerable and rapid changes following interaction with biological fluids and tissues. Alongside this aim, to follow the "destiny" of the polymer is extremely important under a toxicological point of view: this is

particularly relevant when the target is represented by the posterior segment of the eye, because in this case a contact between the polymer and the retina can be envisaged.

Thus, the idea behind this work was to identify a micellar formulation with the ability to solubilize a relevant amount of cyclosporine and promote its transport across ocular barriers. Non-ionic amphiphilic polymers used for micelles preparation were tocopherol polyethylene glycol 1000 succinate (TPGS) and Solutol® HS15. Furthermore, the addition of alpha-linolenic acid was assessed, in the light of the interesting results reported on fatty acids for micelles preparation [25, 26] and increased drug loading [27, 28]. A second aim was to evaluate micelles fate in the ocular tissues (cornea and sclera) to shed light on the penetration mechanisms. This was possible by quantifying both drug and polymer in the tissues, by studying TPGS hydrolysis in a bio-relevant environment and by following micelles penetration with two-photon microscopy.

2. Materials and methods

2.1. Materials

Cyclosporine A (MW 1202.6 g/mol; logP 3; water solubility 27.67 µg/ml [29]) was purchased from Alfa Aesar (Kandel, Germany) while tocopheryl polyethylene glycol 1000 succinate (TPGS) was received from PMC ISOCHEM (Vert-Le-Petit, France). Alpha-linolenic acid (LA; MW 278.43 g/mol; logP 6.46; pK_a 4.77), fluorescein sodium (MW 376.28 g/mol) and Nile red (NR; 9-(diethylamino)-5H-benzo[a]phenoxazin-5-one; MW 318.4 g/mol) were purchased from Sigma-Aldrich (Saint Louis, MO, USA). Solutol® HS15 was received from BASF (Ludwigshafen, Germany) whereas citric acid and propylene glycol were purchased from A.C.E.F. S.p.a (Fiorenzuola d'Arda, Italy). For HPLC analysis high purity water (Purelab® Pulse, Elga Veolia,UK) and HPLC grade acetonitrile were used. Acetate buffer was prepared by mixing 0.1 M acetic acid and 0.1 M sodium acetate solutions in 82:18 (v/v) ratio; pH was adjusted to 4.8 using 0.1 M NaOH. Simulated tear fluid (STF) was obtained by solubilizing in water $CaCl_2$ 0.06 g/l, $NaHCO_3$ 2.18 g/l and NaCl 6.7 g/l; pH was adjusted to 7.4 using 1M HCl. Phosphate Buffer Saline (PBS) was prepared by dissolving in high purity water KH_2PO_4 0.19 g/l, Na_2HPO_4 2.37 g/l and NaCl 8.8 g/l; pH was adjusted to 7.4 using H_3PO_4 85%. HEPES buffer was prepared by solubilizing in high purity water HEPES 5.96 g/l and NaCl 9 g/l; pH was adjusted to 7.4 using NaOH 5M.

2.2. Cyclosporine and linolenic acid quantification method

Cyclosporine and linolenic acid quantification was performed using an HPLC-UV system (Infinity 1260, Agilent Technologies, Santa Clara, CA, USA), with a reverse-phase column (Aeris™ WIDEPORE XB-C_8 column, 150 x 4,60 mm, 3,6 µm, Phenomenex, Torrance, CA, USA) thermostated at 65°C. The mobile phase was composed of CH_3CN:water with TFA 0.1% in ratio 55:45 (v/v). The flow was maintained at 1.6 ml/min and the injection volume was equal to 100 µl. The retention time of cyclosporine and linolenic acid, both quantified by UV absorbance at 230 nm, was respectively of 4.9 and 3.1 minutes. For cyclosporine, linearity was found in the interval 1-50 µg/ml, whereas for

linolenic acid in the range 5-100 µg/ml. Details on calibration curves, RSD%, RE% and LOQ values, as well as discussion on the method and the impact of the injection solvent are reported in the supplementary materials (see par. 1.1).

2.3. TPGS quantification method

TPGS quantification, performed with a previously validated method [30], was done using an HPLC-UV system (Infinity 1260, Agilent Technologies, Santa Clara, CA, USA), with a reverse-phase C18 column (Waters, Symmetry300 C18, 5 µm, 4.6 × 250 mm) and a C18 guard column (SecurityGuard Widepore C18, Phenomenex, Torrance, CA, USA), thermostated at 40 °C. The mobile phase, composed of acetate buffer pH 4.8:CH_3OH in 3:97 (v:v) ratio, was pumped at 2 ml/min. The retention time of TPGS, quantified by UV absorbance at 215 nm, was 4 minutes while the injection volume was 100 µl. Calibration curves were built in the concentration interval 1-25 µg/ml. Samples were injected without previous dilution. Further information on the preparation of the standards for the calibration curve are reported in the supplementary materials (see par. 1.2).

2.4. Preparation of blank polymeric micelles

Polymeric micelles were prepared by direct dissolution of TPGS and/or Solutol® HS15 in high purity water to obtain formulations S (Solutol®), ST (Solutol® and TPGS) and T (TPGS) (see Figure 1 for details on the structure and table 1 for details on the composition of micellar formulations).

Figure 1: Drug and excipients used for micelles preparation with their main chemical features and molecular structure.

Compound	Molecular weight (g/mol)	Log P	HLB	pK_a	H-bond capacity (donor-acceptor)	Molecular structure
Cyclosporine	1202.6	2.92	-	13.3	5-12	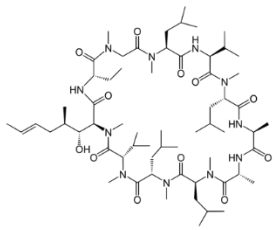
TPGS	1513	-	13.2	-	1-6	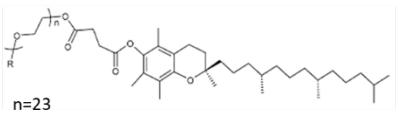
Solutol® HS15	963.2	-	14-16	-	3-19	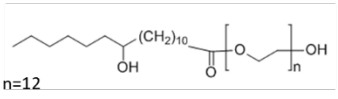
Linolenic acid	278.4	6.46	-	4.77	1-2	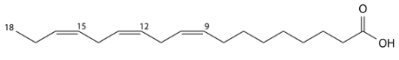

8 ml of S, ST and T micelles were then added with 100 µl of linolenic acid (L) this becoming SL, STL, TL, respectively, and vortexed (3 times x 20 sec each) in order to ensure complete saturation of the aqueous phase. Afterwards, to separate linoleic acid and obtain a clear solution, the oily phase was removed by 2-folds filtration (regenerated cellulose, Sartorius Minisart RC 0.2 µm). The amount of

linolenic acid loaded in the micelles was then evaluated by HPLC after proper dilution with the mobile phase.

Table 1: Blank micellar formulations with relative composition and codification.

CODE	TPGS (mM)	SOLUTOL® HS15 (mM)	LINOLENIC ACID
T	20	-	-
S	-	20	-
ST	10	10	-
TL	20	-	at saturation
SL	-	20	at saturation
STL	10	10	at saturation

2.5. Cyclosporin-loaded polymeric micelles

In order to determine cyclosporine solubility, the blank micellar formulations (see table 1 for the compositions) were added with an excess of the drug, sonicated for 3 minutes and left under magnetic stirring at room temperature for at least 72 h. Then, the suspension was centrifuged at 10,000 rpm for 15 minutes and, when needed, for other 20 minutes at 15,000 rpm to get complete precipitation of the undissolved drug and obtain a limpid formulation. The supernatant was sampled and analyzed by HPLC-UV for determining the solubility of both cyclosporine and linolenic acid after proper dilution with the mobile phase. Cyclosporine solubility is reported as mean ± SD; $n \geq 9$ for T micelles, $n \geq 3$ for the other formulations.

Size and polydispersity index (PDI) of blank and CYC-loaded micelles were measured by Dynamic Light Scattering (DLS) using a Zetasizer Nano-ZSP (Malvern Instruments, Malvern, UK). Measurements were performed at 25 °C after 10-folds dilution in high purity water.

2.6. Tissue preparation

Fresh porcine eyes were isolated from Landrance and Large White (age 10–11 months, weight 145–190 kg), female and male animals supplied from a local slaughterhouse (Macello Annoni S.p.A., Parma, Italy). The eyes were kept in PBS at 4 °C until the dissection, which occurred within 2 h from the enucleation. The muscular and connective tissues around the eye bulb were completely removed. For corneal permeation experiments, only bulbs with macroscopically intact corneas were used, whereas eyes showing opaque corneas were discarded. The cornea, isolated as a corneo-scleral button-shaped piece, was obtained cutting with a scalp beyond the limbus. For scleral permeation, the isolated sclera was obtained by circumferentially cutting and removal of the anterior segment of the eye behind the limbus. The collected eyecup was then cut and everted. The neural retina and the choroid-Bruch's layer were discarded while the sclera was used for the permeation experiment.

2.7. Study of the effect of TPGS on cornea permeability: transcorneal permeation of fluorescein

In order to evaluate if TPGS induces an increase of corneal permeability, the permeation of sodium fluorescein was evaluated after application of TPGS micelles to the tissue for 10 minutes. The tissue was mounted on a glass Franz-type vertical diffusion cell (DISA, Milano, Italy) with a permeation area of 0.2 cm^2. The receptor was filled with HEPES buffer pH 7.4 (about 4 ml, exactly measured) magnetically stirred at 37°C to guarantee sink conditions. First, the donor was pre-treated with 200 µl of TPGS 20 mM micelles for 10 min. Afterwards, the formulation was removed and the tissue was washed 3 times with 200 µl of HEPES buffer and carefully dried with a cotton swab. A solution of fluorescein sodium (1.18 mg/ml) was then applied at infinite dose (200 µl/cm^2) for 4 h. 300 µl of receptor solution were sampled at different timepoints (0, 1, 1.5, 2, 3 and 4 hours from the deposition of the formulation) and the receptor was filled with fresh HEPES buffer. Negative and positive controls were also evaluated. The negative control was represented by a pre-treatment of 10 minutes with HEPES buffer (pH 7.4). The positive control was represented by a 0.1% p/v benzalkonium chloride solution applied for 5 or 10 minutes.

The samples fluorescence (λ_{exc}=490 nm, λ_{em}=535 nm) was measured via microplate reader (SPARK10 M, TECAN, Mannendorf, CH). More information on the preparation of the calibration curve, RSD%, RE% and LOQ values are reported in the supplementary materials (par. 1.3). All experiments were carried out using different ocular bulbs from different animals. The amount of fluorescein sodium permeated (µg/cm^2) was reported as a function of time (min). The transcorneal flux across the cornea (J, µg/cm^2h) was determined as the slope of the regression line at the steady state, while the apparent permeability coefficient (P, cm/s) was calculated at the steady state as: $P=J/C_d$, where C_d (µg/ml) is the concentration of the donor solution. Data are reported as mean ± SD; number of replicates was n ≥ 3, unless differently indicated.

2.8. Retention and permeation experiments across cornea and sclera

The tissue was mounted on a glass Franz-type vertical diffusion cell (DISA, Milano, Italy) with a permeation area of 0.2 cm^2 (cornea) or 0.6 cm^2 (sclera). The set-up used for corneal permeation experiments was previously validated to guarantee that tissue barrier properties were preserved throughout the experiment duration [31]. The receptor was filled with PBS pH 7.4 (4 ml, exactly measured) that was magnetically stirred to guarantee sink conditions. The formulations were applied at infinite dose (200 µl/cm^2, occluded). At the end of the experiment, the receptor solution was sampled, the formulation was removed from the donor and the tissue was rinsed 3 times with PBS. Therefore, cyclosporine and TPGS were extracted by treating tissues with 1 ml solution of CH_3CN:CH_3COOH 1% in 87:13 ratio. Samples were left under these conditions overnight at room temperature, then sonicated for 12 minutes and centrifuged at 12,000 rpm for 15 min before HPLC analysis. This extraction method, previously validated for cyclosporine [30], was also challenged for its ability to extract TPGS. The percentage of recovery found for TPGS was 91.9 ± 3.15 %. In case of cornea, experiment duration was 5 h and CYC-loaded formulations tested were T, TL and ST (see the composition in Table 1 and CYC solubility in Figure 2). In case of sclera, only T was evaluated. The experiments were performed for 6 and 48 h. Additionally, to evaluate the reservoir effect of the tissue, T was applied to the sclera for 6 h; then, the formulation was carefully removed, the sclera surface was dried with a cotton bud and permeation experiment was continued up to 48 h. After

this time, cyclosporine was extracted from the sclera and quantified in the receptor phase, as previously described. Data are reported as mean ± SD; n ≥ 3 for all formulations.

2.9. Hydrolysis of TPGS in contact with ocular tissues

The in vitro enzymatic hydrolysis of TPGS was evaluated using cornea and sclera excised from fresh porcine eyes. In particular, the isolated tissues were punch-biopsied with a 0.9 mm punch and cut in four pieces of the same size.

A solution of TPGS with concentration 100 µg/ml was prepared by dissolving the polymer in a mixture of PBS pH 7.4:water in ratio 1:10. Then, 300 µl of TPGS 100 µg/ml were incubated with two pieces of the tissue (average weight 50 mg for cornea and 60 mg for sclera) for 24 h (for the cornea) and 48 h (for the sclera) at 37°C. At predetermined time intervals, samples were centrifuged at 12,500 rpm for 5 minutes and 40 µl of the TPGS solution were withdrawn and diluted 1:10 with CH_3CN:CH_3COOH 1% (87:13), causing esterase inactivation. The concentration of TPGS in these samples was measured by HPLC. Control samples obtained in the same conditions but without tissue were analyzed as well.

2.10. Two-photon microscopy

For the two-photon microscopy analysis, Nile red-loaded TPGS 20 mM micelles were prepared. Briefly, 10 µl of a 10 mg/ml NR solution in DMSO were added to 1.5 ml of blank TPGS 20 mM micelles. The sample was then centrifuged at 13,000 rpm for 5 min to precipitate the exceeding NR and to collect the supernatant. Afterwards, the corneal or the scleral tissue was mounted on a Franz-type vertical diffuse cell (0.6 cm^2). The donor was filled with 120 µl of NR-loaded TPGS micelles, while the receptor was filled with PBS pH 7.4 under magnetic stirring. The experiment duration was 2 h. The same experiment was performed also using a reference NR saturated aqueous solution prepared by adding 10 µl of a 10 mg/ml NR solution in DMSO to 1.5 ml of high purity water and centrifuging following the conditions previously reported to collect the supernatant.

Porcine samples were analyzed with a Two-Photon Microscope Nikon A1R MP+ Upright equipped with a femtosecond pulsed laser Coherent Chameleon Discovery (~ 100 fs pulse duration with 80 MHz repetition rate, tunable excitation range 660-1320 nm). A 25× water dipping objective with numerical aperture 1.1 and 2-mm working distance was employed for focusing the excitation beam and for collecting the two-photon excited fluorescence (TPEF) and the second harmonic generation (SHG) signals. TPEF/SHG signal was directed by a dichroic mirror to a series of three non-descanned detectors (high sensitivity GaAsP photomultiplier tubes) allowing fast image acquisition. The three detectors are preceded by optical filters allowing the simultaneous acquisition of three separated channels: blue channel (415–485 nm), green channel (506–593 nm) and red channel (604–679 nm). Imaging overlay of the three channels and processing was performed by the operation software of the microscope. Additionally, a fourth GaAsP photomultiplier detector, connected to the microscope through an optical fiber and preceded by a dispersive element, was used to record the spectral profile of the TPEF/SHG signal (wavelength range 430 to 650 nm with a bandpass of 10 nm).

For microscope observations, performed right after dismounting the tissue from the Franz-type cell, the samples were placed in a dedicated plexiglass holder and saline solution was used to dip the objective and to avoid dehydration. Two different excitation wavelengths were used, 860 or 1080 nm. Images were acquired with a typical field of view of 500 µm × 500 µm, except where explicitly reported.

Besides two-photon microscopy analysis, the emission spectrum of NR-loaded TPGS micelles and a NR solution in water were registered with an Edinburgh FLS-1000 fluorimeter. The solutions were prepared by adding 20 µL of a 400 µM DMSO NR stock solution in 3 mL of 0.5 mM TPGS micelles or high purity water (final NR concentration 2.7 µM, total percentage of DMSO < 1%) which were then filtered after the preparation (hydrophilic PTFE, AISIMÔ 0.22 µm).

2.11. Statistical analysis

All data presented in text, figures and tables are reported as mean value ± SD. The significance of the differences between the results was assessed using Student's t-test. Differences were considered statistically significant when $p < 0.05$.

3. Results and discussion

Polymeric micelles have demonstrated to be powerful tools to overcome the drawbacks of traditional ocular dosage forms, with particular potentialities for an improved drug administration to the anterior segment of the eye. Indeed, micelles can be used to formulate hydrophobic compounds as aqueous solutions which, applied as eye drops, can easily mix with the lacrimal fluid without causing any vision interference [14, 32].

3.1. Cyclosporine solubility studies

The first part of the work was dedicated to the identification of micellar formulas capable of increasing cyclosporine aqueous solubility, that is very low; in simulated tear fluid we found a solubility lower than 5 µg/ml.

The polymers used were TPGS and Solutol® HS15, alone or combined in a 1:1 molar ratio. TPGS, was selected for the possible release of antioxidant vitamin E via enzymatic hydrolysis [30]. Moreover, this polymer previously demonstrated its permeation enhancing properties for several drugs through the corneal tissue [33-35] probably related also to P-glycoprotein inhibition [36]. Solutol® HS15 was selected considering its capacity to improve hydrophobic drugs solubility [37, 38] and its promising outcomes regarding the enhancement of corneal permeability and retention [39]. Linolenic acid was also added to the micellar formulations (see table 1 for detailed composition and codification) since data previously collected in our laboratory demonstrated the capability of fatty acids to increase the encapsulation of an hydrophobic compound [27]. Additionally, linolenic acid is a precursor of prostaglandin E1, a potent anti-inflammatory agent capable of reducing the ocular inflammation [40], promoting tear production and decreasing DES symptoms [41]. Some studies demonstrated that dietary supplementation with linolenic acid led to a reduction of ocular surface

inflammation in patients with DES [42, 43] and there is also some evidence of omega-3 fatty acids effectiveness when applied topically [44, 45].

TPGS and Solutol® demonstrated a similar capability to dissolve linolenic acid (4 mg/ml). However, their 1:1 mixture reduced linolenic acid solubility by half. Cyclosporine was then added to the micelles; TPGS alone gave the highest cyclosporine solubility (5.26 ± 0.39 mg/ml) and Solutol® the lowest (0.57 ± 0.1 mg/ml). In the presence of linolenic acid, the solubility of cyclosporine decreased (Table 2) regardless the polymers composition. Also the concentration of linolenic acid after cyclosporine loading (Table 2) showed to be markedly reduced by cyclosporine presence; this suggests a competition between the two molecules for the interaction with the micellar core, whose size is relatively small [27]. This result differs from the previously published data on imiquimod, where fatty acids co-encapsulation was used to increase the solubility of this hydrophobic drug into TPGS micelles [27].

Table 2. Solubility of cyclosporine (CYC) and linolenic acid (LA) alone and combined in the micellar formulations. Formulations further evaluated are indicated in bold.

	FORMULATION	CYC SOLUBILITY (mg/ml)	LA SOLUBILITY (mg/ml)
cyclosporine only	T	5.26 ± 0.39	-
	S	0.57 ± 0.1	-
	ST	3.27 ± 0.28	-
linolenic acid only	TL	-	3.82 ± 0.11
	SL	-	4.26 ± 0.32
	STL	-	2.37 ± 0.31
cyclosporine and linolenic acid	TL	3.04 ± 0.52	0.60 ± 0.03
	SL	n.d.	n.d.
	STL	0.53 ± 0.09	1.240.25

Given the results obtained, the formulations T, TL and ST loaded with cyclosporine were selected for further studies, since they guarantee a drug solubility equal or higher than 3 mg/ml and, in the case of TL, also the presence of linolenic acid that can support drug action. Additionally, these formulations were selected also for their stability, evaluated after approx. 2 months as reported in Figure S2.

The size of the drug-loaded micelles, reported in Table 3, is between 13 and 16 nm. Details on DLS analysis including data on discarded formulations and blank micelles are presented in supplementary material (Table S2). The size of TPGS as well as Solutol® micelles demonstrated to be in good agreement with values reported in the literature [46, 47] and minor changes in micelle size were reported after addition of linolenic acid or after cyclosporine loading, despite the increase in the polydispersity index.

3.2. Cyclosporine and TPGS accumulation and retention in ocular tissues

The role of the micellar formulation on drug delivery to the ocular structures has not been fully clarified. An increased solubility, the permeation enhancing properties of the polymer and the uptake of intact micelles seem to concur to the increased drug penetration [48], however, the contribution of each mechanism is difficult to deduce. In fact, given the nature of these nanocarriers, formed by an association of amphiphilic unimers, the study of the interaction with the biological environment is particularly hard. In this paper, to elucidate the micelles behaviour upon contact with the biological barriers, we quantified both drug and polymer (TPGS) inside the ocular structures.

3.2.1. Cyclosporine and TPGS retention into the cornea

Formulations T, TL and ST loaded with CYC at saturation were then applied to the corneal tissue to evaluate their capability to promote drug uptake into the epithelial cells. At the end of the experiment, the drug was extracted from the tissue with a validated method [30]. This method was also challenged for its ability to extract TPGS that can likewise accumulate in the cornea. The results obtained in term of cyclosporine and TPGS accumulation from these formulations are presented in Table 3, while the amount of polymer and drug permeated is not reported as no transcorneal permeation occurred.

Table 3. Composition, size and CYC solubility of the CYC-loaded micellar formulations evaluated on the corneal tissues. Data on drug and TPGS accumulation in the cornea are also reported.

Micelles characteristics				Cyclosporin and TPGS delivery to the cornea	
	Composition	Size (nm) *(PDI)*	Cyclosporine conc. (mg/ml)	Cyclosporine in corneal tissue (μg/cm^2)	TPGS in corneal tissue (μg/cm^2)
T	TPGS 20 mM	12.96 ± 4.03[46] *(0.091)*	5.26 ± 0.39	19.81 ± 4.49	55.92 ± 26.25
TL	TPGS 20 mM saturated with linolenic acid	14.47 ± 4.91 *(0.196)*	3.04 ± 0.52 (linolenic acid: 0.60 ± 0.03)	2.82 ± 1.43	41.05 ± 22.92
ST	TPGS 10 mM and Solutol® 10 mM	15.65 ± 5.90 *(0.213)*	3.27 ± 0.28	2.35 ± 0.66	2.82 ± 0.08

Formulation T outperformed the others, with an amount of drug accumulated about 7-fold higher. Both the addition of linolenic acid (TL) or Solutol® (ST) decreased micelles delivery efficiency. The reason can only partially be attributed to the different drug concentration (5 vs 3 mg/ml), since all the formulations are at the saturation level and the thermodynamic activity is comparable in all cases. The TPGS concentration in the formulation (20 vs 10 mM) can contribute to partially explain the result, since TPGS has widely demonstrated its permeation enhancing capacity resulting from efflux pumps inhibition and also from the ability to interpose between the phospholipidic bilayers of cellular membranes modifying their fluidity [33, 49]. To shed light on micelles permeation mechanisms, we also quantified the amount of TPGS in the cornea. The accumulation of TPGS in the

absence of Solutol® (T and TL) gave high and comparable results, even if ~~showing~~ it presents high variability. The presence of Solutol® markedly decreased TPGS uptake, partially due to the lower concentration (10 vs 20 mM) and potentially also to a lower mobility of TPGS in the presence of mixed micelles, as previously demonstrated in the presence of poloxamers [46].
Since the TPGS:cyclosporine weight ratio in the T micelles is approximately 6:1, the data of corneal retention suggest that the micelles do not penetrate intact in the tissue; the drug is probably released as the micelles come in contact with the epithelial cells. There are however other phenomena to be considered, since TPGS could be metabolised in the tissue (see par 3.3).

Concerning the relevance of the corneal concentration obtained, we can compare our data with the ones previously obtained with the commercial formulation Ikervis®, a cationic nanoemulsion accumulating a cyclosporine amount of 0.60 ± 0.14 μg/cm^2 [30]. Considering the lower concentration of cyclosporin in Ikervis® (1 mg/ml), its performance is comparable with TL and ST, while formulation T markedly enhanced drug uptake. This can be relevant, considering the growing use of cyclosporine for diseases other than DES [50], that could require higher tissue concentration.

3.2.2. Cyclosporine and TPGS diffusion across the sclera from micellar formulations

In the last years, the topical route has been proposed for the administration of therapeutics also to the posterior segment of the eye. This topic is still under investigation: some researchers have actually highlighted the presence of the drug in the retina, but the clinical significance of the concentrations found is still subject of debate. The first barrier encountered by the formulation after topical application is the conjunctiva, which plays a crucial role as it mediates the delivery to the posterior segment (conjunctival–scleral route), but also the nonproductive and undesirable systemic absorption. Cyclosporine permeation across the conjunctiva from TPGS micelles was studied in a previous work [46]. The results highlighted the capability of both drug and TPGS to cross the conjunctival epithelium in significant amount. However, it is worth mentioning that the fast nasolacrimal clearance from the conjunctival sac as well as the systemic uptake mediated by blood and lymphatic vessels reduce the residence time on the eye surface to few minutes, making the achievemt of therapeutic concentrations in the posterior segment unlikely. A possible alternative is a subconjunctival administration, where the formulation is applied on the surface of the sclera. Although this procedure cannot be defined non-invasive, it avoids the most serious side effects connected with the intravitreal injection and, in the presence of a controlled-release formulation, can reduce the administration frequency. Also in this case, several static, dynamic and metabolic barriers strongly reduce drug absorption [51], therefore, in order to achieve therapeutic concentrations at the posterior ~~chamber~~ segment, ~~topical~~ formulations with high concentration of the drug are required.
T micelles, having the higher cyclosporine concentration among the formulations prepared, were selected for further studies regarding scleral accumulation and permeation. The donor was applied for 6 h or 48 h and, at the end of the experiment, both the drug and TPGS were quantified in the receptor phase and inside the scleral tissue. In order to investigate the “reservoir effect” of the scleral tissue (i.e. the capability to accumulate the drug and then slowly release it to the deeper

tissues), the donor was also applied for 6 hours, then removed and the experiment was continued up to 48 h. Results of drug and TPGS accumulation and permeation are listed in Figure 2.

The amount of cyclosporine recovered in the sclera after the 6 h treatment was much higher than in the cornea (87.75 ± 21.69 µg/cm^2 vs. 19.81 ± 4.49 µg/cm^2), in agreement with the different tissue structure, with the sclera being a permeable connective tissue made of collagen fibres. However, also in this case, no drug was detected in the receptor phase after 6 h from donor deposition.

Cyclosporine accumulation increases over time, from 87.75 ± 21.69 µg/cm^2 after 6 h of contact to 304.86 ± 13.39 µg/cm^2 after 48 h of contact. In this last case, it was also detected in the receptor compartment, in a very significant amount. When the donor was applied for 6 h and then removed, the total amount recovered after 48 h was very similar with respect to the 6 h experiment, but with a different distribution: while after 6 h the 100% of the drug was localized in the sclera, after 48 h the 15% permeated the tissue, demonstrating the capability of the sclera to slowly release the drug and/or the micelles into the deeper tissues.

The fate of TPGS was also followed. The amount recovered in the sclera after 6 h was approximately 500 µg/cm^2. Interestingly, when the donor was applied for 6 h and the quantification was made after 48 h, the amount of TPGS decreased to approximately 300 µg/cm^2. This reduction can be attributed to an esterase-mediated hydrolyzation of TPGS with consequent release of vitamin E [30] and will be further studied.

A

Donor appl. time	6 h		48 h
Exp. duration	**6 h**	**48 h**	**48 h**
CYCLOSPORINE			
Retained (µg/cm^2)	87.75 ± 21.69	72.42 ± 9.30	304.86 ± 13.39
Permeated (µg/cm^2)	< LOQ	12.82 ± 0.32	98.60 ± 47.94
CYC TOT (µg/cm^2)	87.75 ± 21.69	85.24 ± 9.61	403.46 ± 59.97
TPGS			
Retained (µg/cm^2)	517.40 ± 220.50	267.44 ± 34.57	1029.09 ± 163.26
Permeated (µg/cm^2)	< LOQ	26.99 ± 11.40	627.03 ± 312.69
TPGS TOT (µg/cm^2)	517.40 ±220.50	294.43 ± 43.46	1656.12 ± 283.79

B

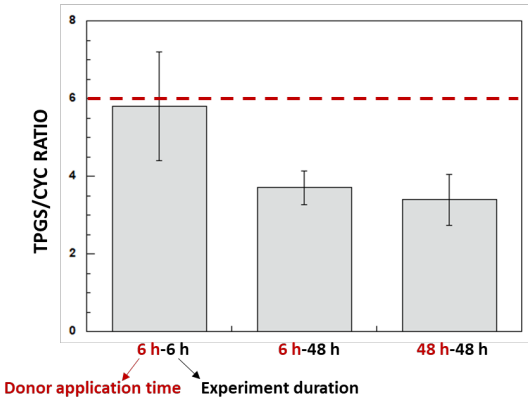

Figure 2. Panel A shows the amount of cyclosporine and TPGS accumulated in the sclera and permeated across the sclera (average ± SD) after formulation application in infinite dose conditions for 6 h and 48 h. The reservoir effect was also evaluated by removing the donor after 6 h and continuing the experiment for up to 48 h. Panel B represents TPGS/CYC ratio related to the amount accumulated inside the sclera following different donor application times and experiment durations. The red line shows the TPGS/cyclosporine ratio (TPGS/CYC) in the T formulation.

The quantification of TPGS gives the possibility of investigating the mechanisms of micelles penetration. The ratio between TPGS (30 mg/ml) and cyclosporine (5 mg/ml) in T micelles is approximately 6 (dotted line in Figure 2B). We have then considered drug and TPGS recovered (accumulated + permeated) at the end of each experiment and calculated this ratio. The result, presented in Figure 2, panel B, shows that the TPGS/cyclosporine ratio of the formulation is maintained in case of 6 h experiment duration suggesting that both the polymer and the drug are permeated together in form of intact micelles. This is reasonable, if considering the small size of this nanocarriers and the relatively high porosity of the sclera. The reduced polymer/drug ratio

registered for the other experimental conditions can be attributed to TPGS hydrolysis taking place in the scleral tissue and particularly evident at long contact times (see par 3.3).

3.3. TPGS metabolism in contact with ocular tissues

Previous studies [30, 52] indicate that TPGS, which is stable in solution between pH 4.5 and 7.5, can be hydrolyzed to vitamin E and vitamin E succinate in the presence of esterases, enzymes ubiquitously present in tissues and also in the porcine [54] and human [53, 55] cornea and sclera. However, at the best of our knowledge, the hydrolysis of TPGS in contact with ocular tissues has never been studied before. This point is relevant since TPGS degradation could cause a reduction or even loss of the micelles self-assembling properties promoting drug release.

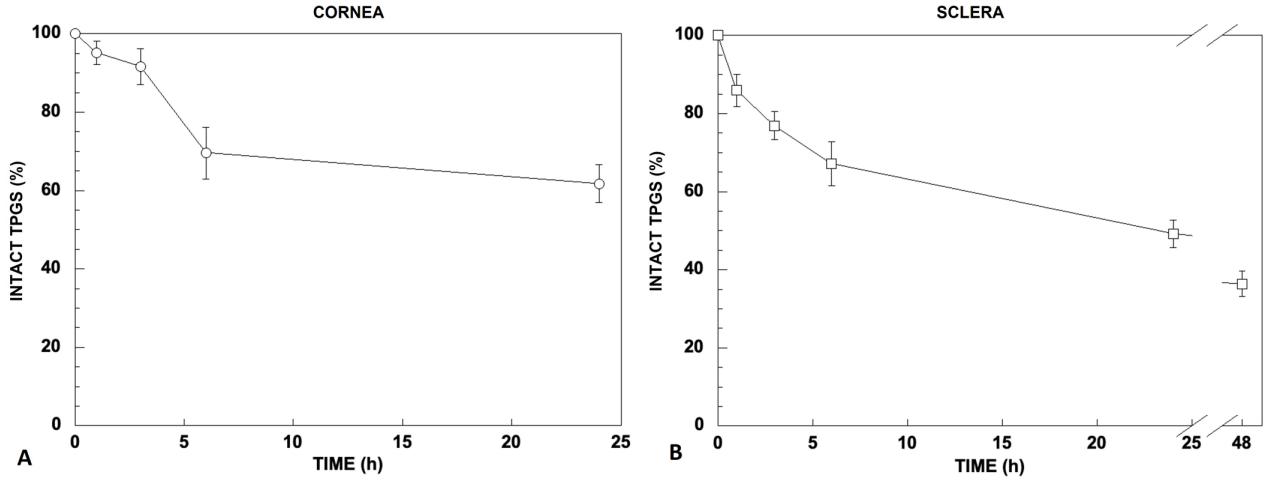

Figure 3. TPGS metabolism in contact with ocular tissues. Panel A: % of intact TPGS recovered after contact with the cornea at 37°C; the ratio between TPGS amount (20 µg) and corneal tissue (approx. 50 mg) was around 0.4 µg/mg of tissue. The data is the mean value of 12 samples from 6 different eyes. Panel B: % of intact TPGS recovered after contact with the sclera at 37°C; the ratio between TPGS amount (30 µg) and scleral tissue (approx. 60 mg) was around 0.5 µg/mg of tissue. The data is the mean value of 12 samples from 4 different eyes.

Overall the results obtained (Figure 3) show a decrease of TPGS concentration in contact with both cornea and sclera. Although the initial partition of the polymer in the tissue, we can reasonably hypothesize that this reduction was due to enzymatic degradation since no TPGS reduction occurred in absence of tissues (control samples) and the HPLC traces highlighted the appearance of vitamin E succinate and vitamin E. The peaks of these metabolites however, were not enough high and resolved to be accurately quantified probably because, differently from the situation were TPGS metabolism was evaluated in solution in the presence of isolated esterase [30], the formed vitamins (lipophilic) can remain stacked in the tissue. Together with the time required to TPGS to penetrate the tissue, the degradation profiles obtained depend on esterase concentration and activity in the two tissues. The faster metabolism in the sclera, clearly visible in the first 3 hours, is in agreement

with literature data on 4-nitrophenyl acetate hydrolysis that highlight a 2-fold faster rate of sclera for comparison with cornea [54].

It is difficult to numerically compare these results with the data obtained in the permeation experiment, given the different conditions in term of TPGS concentration and TPGS/tissue ratio. However, the data collected support the presence of a relatively fast metabolism inside ocular tissue. This could help to explain the data obtained in the transscleral experiment and support cyclosporine release into the tissue owing to TPGS degradation.

It is also worth mentioning that the release of vitamin E and vitamin E succinate, potent antioxidant compounds, could have a positive effect on the treatment of various ocular diseases, although there are still conflicting reports on their efficacy [56, 57].

3.4 Two-photon microscopy of tissues stained with NR-loaded micelles

To further investigate micelles penetration, Nile Red (NR)-loaded TPGS micelles were prepared; their size resulted comparable with the blank micelles. Cornea and sclera were treated for 2 hours with the NR-loaded micelles and the tissues were then imaged with two-photon microscopy with an irradiation wavelength of 860 or 1080 nm. As reference, a saturated aqueous solution of NR was used. NR was selected due to the very poor water-solubility ~~(as cyclosporine)~~; additionally, its emission spectrum is sensitive to the environment polarity [58]. NR, despite being a lipophilic probe, has notable differences in structure and MW if compared to cyclosporine. This means that we cannot claim that the behavior of NR-loaded micelles will be exactly the same as the drug-loaded micelles. However, the data obtained with NR can contribute to understand the behavior of micelles, when combined with the results obtained using all other techniques.

3.4.1. Two-photon microscopy of corneal tissue stained with NR-loaded micelles

Two-photon microscopy is an advanced technique, allowing for in-depth 3D visualization of biological tissues without sample handling (*i.e.* fixation, processing, sectioning, staining). In fact, the specimen is simply fit into a sample holder, moistened with saline solution to avoid dehydration, and immediately observed. In addition, in comparison to conventional fluorescence or confocal microscopy, two-photon microscopy uses less energetic photons (in the red and near-infrared region) thus reducing the photodamage that is instead typically caused by UV and visible light. Finally, specific asymmetric structures (*e.g.* collagen fibers) can be selectively imaged exploting the process of second-harmonic generation [59]. Figure 4 collects the images of the corneal epithelium and the upper stroma after 2 hours treatment with NR-loaded micelles and with a reference NR aqueous solution, when excited at 860 nm. In these conditions, NR is mainly detected in the red channel, while the corneal epithelium gives an autofluorescence signal which falls primarily in the green spectral region. The stroma is blue, due to the second harmonic generation signal (that falls at 430 nm at this excitation wavelength) typical of collagen fibers [60], while the presence of fibroblasts is clearly marked by NR accumulation.

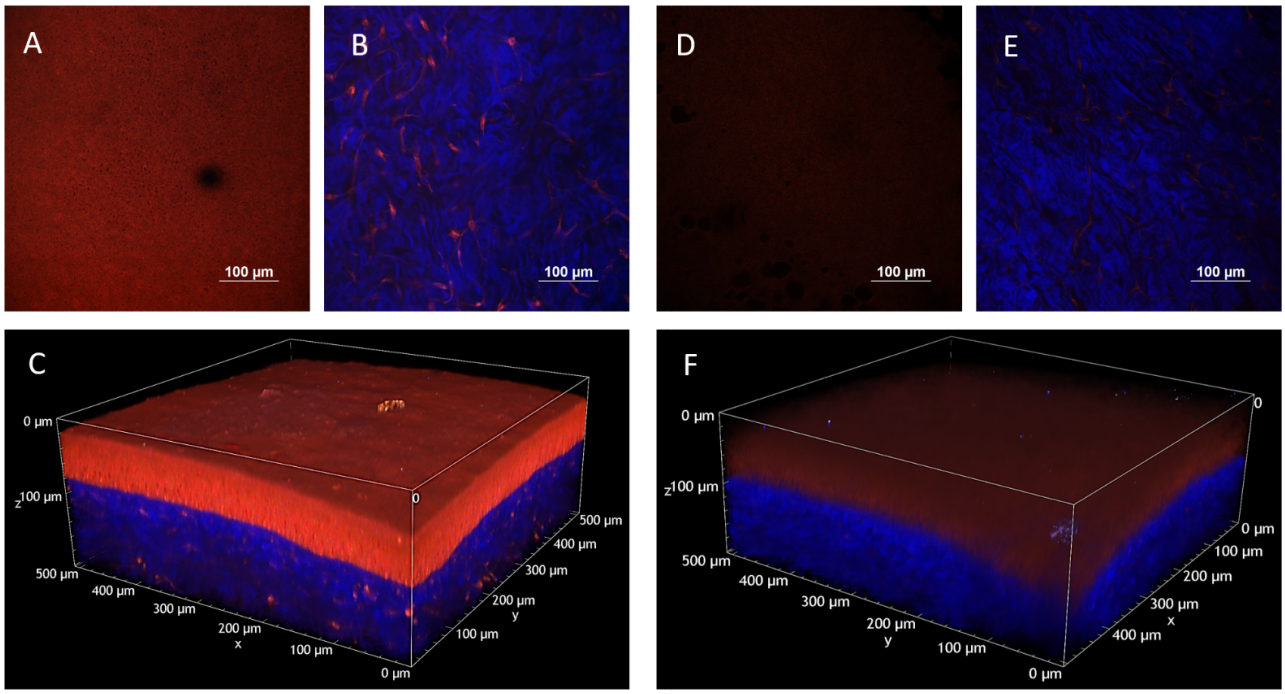

Figure 4. Volume renderings of corneal tissue (epithelium side) reconstructed from Z-stack, acquired with an excitation wavelength of 860 nm (SHG from collagen in blue, NR fluorescence detected in both red and green channels). Panel A-C: sample treated with TPGS micelles loaded with NR (Z-step: 1 µm, total depth: 202 µm). Panels A and B: XY scans collected at 40 and 300 µm depth, respectively; panel C: 3D overview; Panel D-F: reference treated with NR saturated aqueous solution (Z-step: 1 µm, total depth: 202 µm). Panels D and E: XY scans collected at 40 and 300 µm depth, respectively, panel F: 3D overview. All the images in the two Z-scans were acquired with the same detector gains and laser power.

The intensity of NR signal obtained with the micelles is much higher compared to the reference solution, due to the higher fluorescent probe concentration. Similar results were obtained when imaging the endothelial side of the tissues (Figure S3).

In order to obtain information on micelles-tissue interaction, we acquired emission spectra from the tissue at specific focal planes. In fact, being NR a solvatochromic probe [58], the position of its emission spectrum changes with the polarity of the environment. This permits to differentiate between NR included in the micellar core and NR released and consequently located in cells and/or in the intercellular matrix. Spectra were collected exciting the sample at 1080 nm, in order to minimize the tissue autofluorescence and maximize at the same time the NR signal.

In Figure 5, the emission spectrum of NR in TPGS micelles (black dashed line) is compared with the one collected from a corneal sample treated with micelles at a depth of 40 µm (i.e. in the epithelium, corresponding to the image in Figure 4A) and 300 µm (i.e. in the corneal stroma, corresponding to the image Figure 4B) from the corneal surface. The emission spectrum collected from the tissue is shifted toward shorter wavelengths, and the shift increases with increasing depth. The observed shift suggests that the probe is located in an environment having a different polarity with respect to the micelles, indicating NR release from the nanocarrier. This conclusion is further supported by the spectrum obtained from the tissue treated with a NR aqueous solution (green line), which is superimposable with the spectrum obtained from the tissue treated with micelles (Figure 5 and supplementary material Figure S4), confirming that NR is released from the nanocarrier.

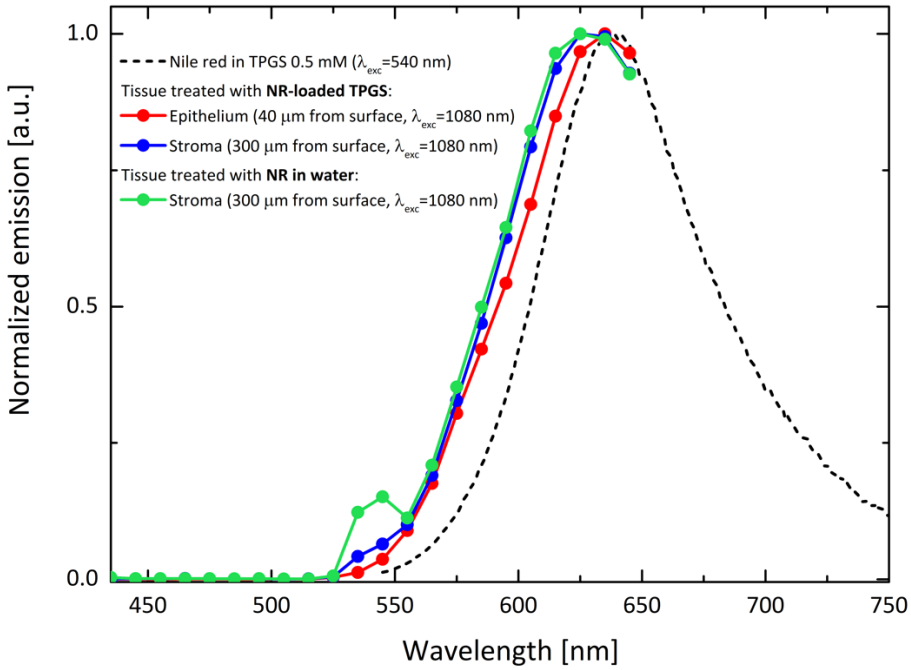

Figure 5. Comparison of the emission spectra recorded in the tissue in correspondence of the epithelium (40 µm from surface, red line) and the stroma (300 µm from surface, NR-loaded TPGS: blue line, NR in water: green line) with the emission profile of an aqueous solution of NR-loaded TPGS micelles recorded with a fluorometer (black dashed line).

The results indicate micelles disassembling in contact with the cornea, in agreement with the data of TPGS and cyclosporine corneal retention discussed in par. 3.2.1.

3.4.2. Two-photon microscopy of scleral tissue stained with NR-loaded micelles

Figure 6 reports images obtained from a scleral sample treated for 2 hours with NR-loaded micelles, upon irradiation at 860 nm. Collagen fibers appear in blue as a result of their second harmonic generation (SHG) signal [61], while the red signal is given by NR fluorescence.

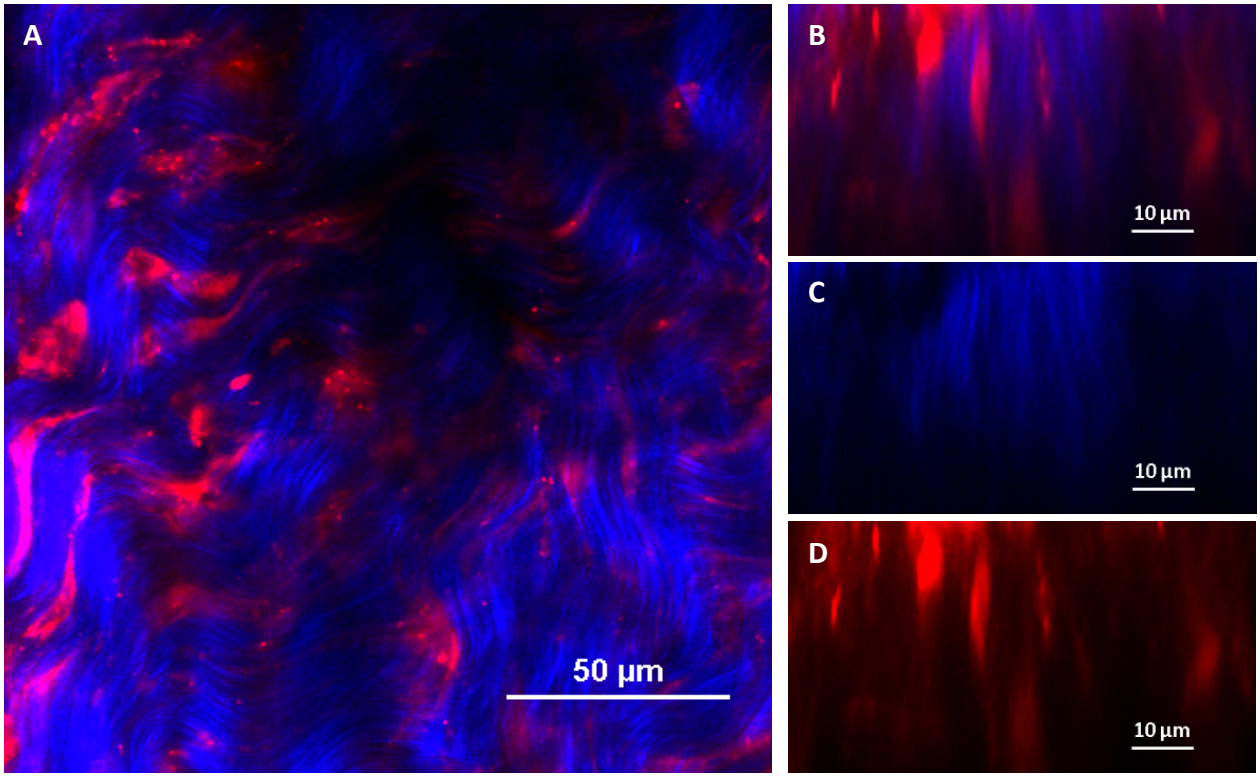

Figure 6. Panel A represents the scleral structure (XY plane) after treatment with NR-loaded micelles when irradiated at 860 nm (SHG from collagen in blue, NR fluorescence in red). Panel B (blue and red channels overlay), C (blue channel) and D (red channel) represent XZ views of scleral collagen fibers extracted from a Z-stack (image size: 77 µm x 39 µm, Z step: 0.42 µm).

As shown in figure 6 panel B, C and D, there is no overlap between the blue and red signals, demonstrating that the fluorescent dye arranges in the interfibrillar spaces. Images were collected also upon excitation at 1080 nm and again the signals of collagen fibers and NR were complementary (Figure S5 in the supplementary materials).

As previously described for the cornea, to get further insight into micelles penetration mechanism, emission spectra were recorded from the tissue. First of all, differently from the cornea, the emission profile recorded from the scleral tissue after micelles application is superimposable with the emission spectrum of micelles in solution (see Figure 7), indicating that the probe has not been released and micelles diffuse in their intact form inside the scleral pore. Indeed, the interaction with a cellular tissue such as the cornea affects micelles integrity much more than a collagen-based structure such as the sclera. When the aqueous NR solution was applied to the sclera, the spectrum obtained was clearly shifted toward higher wavelengths (Figure 7), indicating a more hydrophilic environment, in agreement with the presence of hydrated glycosaminoglycans in the interfibrillar spaces. Indeed, the profile is very similar to the one obtained with a spectrofluorometer from an aqueous solution of the dye.

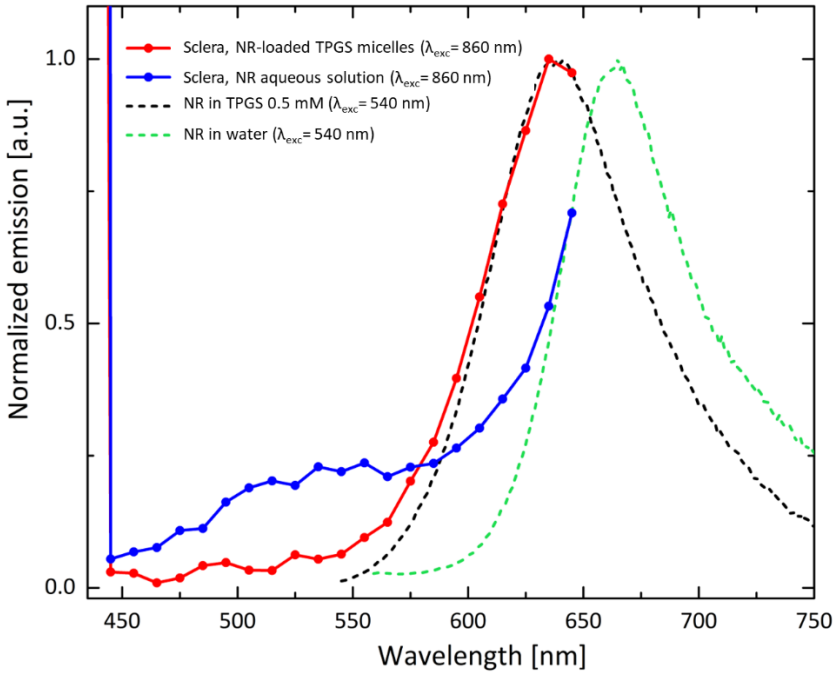

Figure 7: Emission spectrum (excitation at 860 nm) recorded in the sclera (100 µm from surface) after treatment with NR-loaded TPGS micelles (red line) or the NR saturated aqueous solution (blue line); emission spectrum of NR-loaded TPGS micelles (black dashed line) and NR in water (green dashed line). The last two emission spectra have been acquired using a fluorimeter.

Apparently, micelles diffuse intact across the hydrated interfibrillar matrix, and this observation is in agreement with the quantification of cyclosporine and TPGS inside the sclera, which highlights that the TPGS/CYC ratio found in the tissue after 6 h of contact corresponds to the one present in the micellar formulation (Figure 2B).

Micelles diffusion occurs in the interfibrillar matrix made of negatively charged hydrated proteoglycans consisting of a protein core with glycosaminoglycan (GAG) sidechains of repeating disaccharide units (chondroitin, dermatan, keratan or heparin sulfate) [62, 63]. Indeed, previous data have demonstrated the ability of TPGS micelles loaded with NR to diffuse intact through a hyaluronic acid gel [27], possibly due to the presence of the pegylated corona [64]. The inner part of the sclera is made up of thinner and more regularly arranged collagen fibers that give rise to a more compact structure [65, 66]. This compact structure, together with the tortuosity of the pores [67], makes it difficult for the micelles to quickly diffuse into the deepest sclera as evidenced by the absence of transscleral penetration of cyclosporine after 6 hours of application; micelles can be slowed down or even get stuck in the sinuous and convoluted pores. However, interaction with the fibers and/or interfibrillar material together with the enzymatic hydrolysis of the TPGS, determines, over a longer time, the release of cyclosporine and its delivery to the underlying tissues.

3.3. Study of the effect of TPGS on cornea permeability: transcorneal permeation of fluorescein

Corneal retentions studies (par 3.2.1) demonstrated the permeation enhancing ability of TPGS. It is however well known that penetration enhancers can also have irritative effects on the epithelium and that an important requisite is linked to the possibility to quickly restore tissue barrier properties.

In this paper, we used the transcorneal flux of a probe, sodium fluorescein, to assess possible changes in the tissue permeability determined by TPGS application. Specifically, the cornea was pre-treated with TPGS 20 mM (i.e. 3% p/v) for 10 minutes, the solution was then removed, the tissue was rinsed and the permeability of sodium fluorescein was measured. As negative control, a pre-treatment of 10 minutes with HEPES buffer was used. As positive control, a concentrated (0.1% p/v) benzalkonium chloride solution was applied.

The permeability coefficients obtained are reported in Table 4. The pre-treatment with HEPES buffer gave a fluorescein permeability coefficient comparable with the previously published data (5.00 ± 4.29 x 10^{-7} cm/s) [31], while the use of a concentrated benzalkonium chloride solution demonstrated to induce a substantial increase in corneal permeability even after only 5 minutes application, in agreement with literature data [68]. TPGS 20 mM gave a permeability coefficient not statistically different from the control, confirming a reversible effect at least after 10 minutes application.

Table 4. Permeability coefficient (x 10^{-7}) cm/s of fluorescein sodium across the sclera after pre-treatment with various excipients.

PRE-TREATMENT	Permeability coefficient (x 10^{-7}) cm/s
HEPES buffer, 10 min	5.01 ± 3.32
TPGS 20 mM (3%), 10 min	9.83 ± 5.05
Benzalkonium chloride 0.1%, 5 min[a]	28.72 ± 1.65**
Benzalkonium chloride 0.1%, 10 min [a]	55.5 ± 2.07**

[a]n=2, **statistically different from the HEPES buffer ($p<0.001$)

This application time was selected to better mimic the *in-vivo* conditions characterized by a limited formulation-tissue contact time. Despite the promising result, the evaluation of the irritation potential is quite complex and can only be performed in vivo and after chronic application. There is however some encouraging evidence on the good tolerability of this polymer, given by the commercialization of medical devices containing this compound (Ribocross®; Coqun®) even if at lower concentration.

3. Conclusion

The combination of permeation/retention data, hydrolysis results, and two-photon microscopy images demonstrated the different interaction between ~~nano~~micelles and the two different tissues. Upon contact with the cornea, micelles disassemble and cyclosporin is probably uptaken as a free molecule. On the contrary, they can penetrate intact into the sclera, at least in the outermost part of the tissue, characterized by larger collagen fibers, organized in rather irregular bundles. The interaction of the micelles with the fibers and with the interfibrillar material together with the enzymatic hydrolysis of the TPGS, determines, in a longer time, the release of cyclosporine and its transscleral diffusion. The transscleral transport of intact micelles to the choroidal side cannot be demonstrated by our data, even if it cannot be completely excluded.

Overall, TPGS micelles are a very interesting vehicle for cyclosporin ocular delivery, since they are a water-based formulation with very low irritation potential. They efficiently promote drug permeation and retention within cornea and sclera and, in the last case, can form a drug reservoir

into the tissue that can sustain drug release into deeper tissues for an extended time. This, together with the relatively high drug concentration, could reduce administration frequency thus increasing patient's compliance. Additionally, TPGS hydrolysis determines vitamin E and vitamin E succinate release, with an antioxidant activity that can potentially contribute to the improvement of oxidation-mediated diseases. Finally, it is worth mentioning the easy preparation procedure, the possibility of sterilization by filtration and the good stability.

Authors contributions

Martina Ghezzi: conceptualization, methodology, investigation, writing-original draft preparation, writing - review and editing; Ilaria Ferraboschi: investigation, writing – review and editing; Andrea Delledonne: methodology, investigation, writing – review and editing; Silvia Pescina: methodology, validation, writing – review and editing; Cristina Padula: validation, writing – review and editing; Patrizia Santi: writing – review and editing, funding acquisition; Cristina Sissa: validation, writing – review and editing, funding acquisition; Francesca Terenziani: methodology, writing – review and editing, funding acquisition; Sara Nicoli: conceptualization, methodology, writing - original draft preparation, writing - review and editing, funding acquisition. All authors have read and agreed to the published version of the manuscript.

Funding

This work was supported by a Grant from the Italian Ministry of Research (Grant PRIN 2017 # 20173ZECCM Tackling biological barriers to antigen delivery by nanotechnological vaccines (NanoTechVax). Andrea Delledonne, Ilaria Ferraboschi, Cristina Sissa and Francesca Terenziani benefited from the equipment and support of the COMP-HUB Initiative, funded by the "Departments of Excellence" program of the Italian Ministry for Education, University and Research (MIUR, 2018–2022). We acknowledge the financial support of the University of Parma (Bando di accesso al Fondo Attrezzature Scientifiche 2018), for the purchase of the two-photon microscopy facility. Ilaria Ferraboschi benefited of a PhD fellowship financed by PON R&I 2014-2020 (FSE REACT-EU fundings). This work has received funding from the European Union's Horizon 2020 research and innovation programme under the Marie Skłodowka-Curie grant agreement No 101007804 (Micro4Nano).

Acknowledgments

Authors gratefully thank Pierugo Cavallini and Macello Annoni SpA for kindly providing porcine eye bulbs. Former undergraduate students Daisy Sorgi, Alessia Filippini and Francesca Di Pancrazio are gratefully acknowledged for their contribution in data collection.

Declaration of competing interest

The authors declare that they have no known competing financial interests or personal relationships that could have appeared to influence the work reported in this paper.

Disclosures

Partially presented (poster) at PBP World Meeting 2022, Rotterdam, 28-31 March 2022: "Micelles-loaded polymeric films to improve cyclosporine solubility and ocular delivery to the posterior segment", M. Ghezzi, S. Pescina, C. Padula, P. Santi, S. Nicoli.

References:

[1] M. Krönke, W.J. Leonard, J.M. Depper, S.K. Arya, F. Wong-Staal, R.C. Gallo, T.A. Waldmann, W.C. Greene, Cyclosporin A inhibits T-cell growth factor gene expression at the level of mRNA transcription, Proceedings of the National Academy of Sciences, 81 (1984) 5214.

[2] V. Gupta, P.K. Sahu, Topical cyclosporin A in the management of vernal keratoconjunctivitis, Eye, 15 (2001) 39-41.

[3] S. Tatlipinar, E.K. Akpek, Topical ciclosporin in the treatment of ocular surface disorders, The British journal of ophthalmology, 89 (2005) 1363-1367.

[4] S.N. Rao, Comparison of the Efficacy of Topical Cyclosporine 0.05% Compared With Tobradex for the Treatment of Posterior Blepharitis, Investigative Ophthalmology & Visual Science, 46 (2005) 2662-2662.

[5] M. Rubin, S.N. Rao, Efficacy of Topical Cyclosporin 0.05% in the Treatment of Posterior Blepharitis, Journal of Ocular Pharmacology and Therapeutics, 22 (2006) 47-53.

[6] A.T. Vitale, A. Rodriguez, C.S. Foster, Low-dose Cyclosporin A Therapy in Treating Chronic, Noninfectious Uveitis, Ophthalmology, 103 (1996) 365-374.

[7] R.J. Barry, Q.D. Nguyen, R.W. Lee, P.I. Murray, A.K. Denniston, Pharmacotherapy for uveitis: current management and emerging therapy, Clinical ophthalmology (Auckland, N.Z.), 8 (2014) 1891-1911.

[8] Z. Saleh, T. Arayssi, Update on the therapy of Behçet disease, Therapeutic Advances in Chronic Disease, 5 (2014) 112-134.

[9] F. Lallemand, O. Felt-Baeyens, K. Besseghir, F. Behar-Cohen, R. Gurny, Cyclosporine A delivery to the eye: A pharmaceutical challenge, European Journal of Pharmaceutics and Biopharmaceutics, 56 (2003) 307-318.

[10] N. El Tayar, A.E. Mark, P. Vallat, R.M. Brunne, B. Testa, W.F. van Gunsteren, Solvent-dependent conformation and hydrogen-bonding capacity of cyclosporin A: evidence from partition coefficients and molecular dynamics simulations, Journal of Medicinal Chemistry, 36 (1993) 3757-3764.

[11] F. Lallemand, M. Schmitt, J.-L. Bourges, R. Gurny, S. Benita, J.-S. Garrigue, Cyclosporine A delivery to the eye: A comprehensive review of academic and industrial efforts, European Journal of Pharmaceutics and Biopharmaceutics, 117 (2017) 14-28.

[12] A. Patel, K. Cholkar, V. Agrahari, A.K. Mitra, Ocular drug delivery systems: An overview, World journal of pharmacology, 2 (2013) 47-64.

[13] M. Ghezzi, S. Pescina, C. Padula, P. Santi, E. Del Favero, L. Cantù, S. Nicoli, Polymeric micelles in drug delivery: An insight of the techniques for their characterization and assessment in biorelevant conditions, Journal of Controlled Release, 332 (2021) 312-336.

[14] Polymeric micelles for ocular drug delivery: From structural frameworks to recent preclinical studies, Journal of Controlled Release, 248 (2017) 96 - 116.

[15] M.A. Toscanini, M.J. Limeres, A.V. Garrido, M. Cagel, E. Bernabeu, M.A. Moretton, D.A. Chiappetta, M.L. Cuestas, Polymeric micelles and nanomedicines: Shaping the future of next generation therapeutic strategies for infectious diseases, Journal of Drug Delivery Science and Technology, 66 (2021) 102927.

[16] M.A. Grimaudo, S. Pescina, C. Padula, P. Santi, A. Concheiro, C. Alvarez-Lorenzo, S. Nicoli, Topical application of polymeric nanomicelles in ophthalmology: a review on research efforts for the noninvasive delivery of ocular therapeutics, Expert Opinion on Drug Delivery, 16 (2019) 397-413.
[17] Y. Yu, D. Chen, Y. Li, W. Yang, J. Tu, Y. Shen, Improving the topical ocular pharmacokinetics of lyophilized cyclosporine A-loaded micelles: formulation, in vitro and in vivo studies, Drug delivery, 25 (2018) 888-899.
[18] A. Varela-Garcia, A. Concheiro, C. Alvarez-Lorenzo, Soluplus micelles for acyclovir ocular delivery: Formulation and cornea and sclera permeability, International Journal of Pharmaceutics, 552 (2018) 39-47.
[19] Z. Li, M. Liu, L. Ke, L.-J. Wang, C. Wu, C. Li, Z. Li, Y.-L. Wu, Flexible polymeric nanosized micelles for ophthalmic drug delivery: research progress in the last three years, Nanoscale Advances, 3 (2021) 5240-5254.
[20] C. Di Tommaso, J.-L. Bourges, F. Valamanesh, G. Trubitsyn, A. Torriglia, J.-C. Jeanny, F. Behar-Cohen, R. Gurny, M. Möller, Novel micelle carriers for cyclosporin A topical ocular delivery: In vivo cornea penetration, ocular distribution and efficacy studies, European Journal of Pharmaceutics and Biopharmaceutics, 81 (2012) 257-264.
[21] R.D. Vaishya, M. Gokulgandhi, S. Patel, M. Minocha, A.K. Mitra, Novel Dexamethasone-Loaded Nanomicelles for the Intermediate and Posterior Segment Uveitis, AAPS PharmSciTech, 15 (2014) 1238-1251.
[22] N. Elsaid, S. Somavarapu, T.L. Jackson, Cholesterol-poly(ethylene) glycol nanocarriers for the transscleral delivery of sirolimus, Experimental Eye Research, 121 (2014) 121-129.
[23] C. Peng, L. Kuang, J. Zhao, A.E. Ross, Z. Wang, J.B. Ciolino, Bibliometric and visualized analysis of ocular drug delivery from 2001 to 2020, Journal of Controlled Release, 345 (2022) 625-645.
[24] Polymeric micelles in mucosal drug delivery: Challenges towards clinical translation, Biotechnology Advances, 33 (2015) 1380 - 1392.
[25] Y. Wang, L. Jiang, Q. Shen, J. Shen, Y. Han, H. Zhang, Investigation on the self-assembled behaviors of C18 unsaturated fatty acids in arginine aqueous solution, RSC Advances, 7 (2017) 41561-41572.
[26] A.-L. Fameau, A. Arnould, A. Saint-Jalmes, Responsive self-assemblies based on fatty acids, Current Opinion in Colloid & Interface Science, 19 (2014) 471-479.
[27] M. Ghezzi, S. Pescina, A. Delledonne, I. Ferraboschi, C. Sissa, F. Terenziani, P.D.F.R. Remiro, P. Santi, S. Nicoli, Improvement of Imiquimod Solubilization and Skin Retention via TPGS Micelles: Exploiting the Co-Solubilizing Effect of Oleic Acid, Pharmaceutics, 13 (2021) 1476.
[28] S. Tampucci, L. Guazzelli, S. Burgalassi, S. Carpi, P. Chetoni, A. Mezzetta, P. Nieri, B. Polini, C.S. Pomelli, E. Terreni, D. Monti, pH-Responsive Nanostructures Based on Surface Active Fatty Acid-Protic Ionic Liquids for Imiquimod Delivery in Skin Cancer Topical Therapy, Pharmaceutics, 12 (2020) 1078.
[29] G. Ismailos, C. Reppas, J.B. Dressman, P. Macheras, Unusual solubility behaviour of cyclosporin A in aqueous media, Journal of Pharmacy and Pharmacology, 43 (1991) 287-289.
[30] M.A. Grimaudo, S. Pescina, C. Padula, P. Santi, A. Concheiro, C. Alvarez-Lorenzo, S. Nicoli, Poloxamer 407/TPGS Mixed Micelles as Promising Carriers for Cyclosporine Ocular Delivery, Mol Pharm, 15 (2018) 571-584.
[31] S. Pescina, P. Govoni, A. Potenza, C. Padula, P. Santi, S. Nicoli, Development of a Convenient ex vivo Model for the Study of the Transcorneal Permeation of Drugs: Histological and Permeability Evaluation, Journal of Pharmaceutical Sciences, 104 (2015) 63-71.

[32] R.D. Bachu, P. Chowdhury, Z.H.F. Al-Saedi, P.K. Karla, S.H.S. Boddu, Ocular Drug Delivery Barriers—Role of Nanocarriers in the Treatment of Anterior Segment Ocular Diseases, Pharmaceutics, 10 (2018) 28.
[33] C. Ostacolo, C. Caruso, D. Tronino, S. Troisi, S. Laneri, L. Pacente, A. Del Prete, A. Sacchi, Enhancement of corneal permeation of riboflavin-5'-phosphate through vitamin E TPGS: A promising approach in corneal trans-epithelial cross linking treatment, International Journal of Pharmaceutics, 440 (2013) 148-153.
[34] M.H. Warsi, M. Anwar, V. Garg, G.K. Jain, S. Talegaonkar, F.J. Ahmad, R.K. Khar, Dorzolamide-loaded PLGA/vitamin E TPGS nanoparticles for glaucoma therapy: Pharmacoscintigraphy study and evaluation of extended ocular hypotensive effect in rabbits, Colloids and Surfaces B: Biointerfaces, 122 (2014) 423-431.
[35] M. Alkholief, H. Albasit, A. Alhowyan, S. Alshehri, M. Raish, M. Abul Kalam, A. Alshamsan, Employing a PLGA-TPGS based nanoparticle to improve the ocular delivery of Acyclovir, Saudi Pharmaceutical Journal, 27 (2019) 293-302.
[36] E.-M. Collnot, C. Baldes, M.F. Wempe, R. Kappl, J. Hüttermann, J.A. Hyatt, K.J. Edgar, U.F. Schaefer, C.-M. Lehr, Mechanism of Inhibition of P-Glycoprotein Mediated Efflux by Vitamin E TPGS: Influence on ATPase Activity and Membrane Fluidity, Molecular Pharmaceutics, 4 (2007) 465-474.
[37] A.W.G. Alani, D.A. Rao, R. Seidel, J. Wang, J. Jiao, G.S. Kwon, The Effect of Novel Surfactants and Solutol® HS 15 on Paclitaxel Aqueous Solubility and Permeability Across a Caco-2 Monolayer, Journal of Pharmaceutical Sciences, 99 (2010) 3473-3485.
[38] L. Song, Y. Shen, J. Hou, L. Lei, S. Guo, C. Qian, Polymeric micelles for parenteral delivery of curcumin: Preparation, characterization and in vitro evaluation, Colloids and Surfaces A: Physicochemical and Engineering Aspects, 390 (2011) 25-32.
[39] N.F. Younes, S.A. Abdel-Halim, A.I. Elassasy, Solutol HS15 based binary mixed micelles with penetration enhancers for augmented corneal delivery of sertaconazole nitrate: optimization, in vitro, ex vivo and in vivo characterization, Drug Delivery, 25 (2018) 1706-1717.
[40] P.F. Hoyng, N. Verbey, L. Thörig, N.J. van Haeringen, Topical prostaglandins inhibit trauma-induced inflammation in the rabbit eye, Investigative Ophthalmology & Visual Science, 27 (1986) 1217-1225.
[41] A. Macrì, S. Giuffrida, V. Amico, M. Iester, C.E. Traverso, Effect of linoleic acid and γ-linolenic acid on tear production, tear clearance and on the ocular surface after photorefractive keratectomy, Graefe's Archive for Clinical and Experimental Ophthalmology, 241 (2003) 561-566.
[42] S. Barabino, M. Rolando, P. Camicione, G. Ravera, S. Zanardi, S. Giuffrida, G. Calabria, Systemic Linoleic and γ-Linolenic Acid Therapy in Dry Eye Syndrome With an Inflammatory Component, Cornea, 22 (2003).
[43] I. Molina-Leyva, A. Molina-Leyva, A. Bueno-Cavanillas, Efficacy of nutritional supplementation with omega-3 and omega-6 fatty acids in dry eye syndrome: a systematic review of randomized clinical trials, Acta Ophthalmologica, 95 (2017) e677-e685.
[44] J.S. Fogt, N. Fogt, P.E. King-Smith, H. Liu, J.T. Barr, Changes in Tear Lipid Layer Thickness and Symptoms Following the Use of Artificial Tears with and Without Omega-3 Fatty Acids: A Randomized, Double-Masked, Crossover Study, Clinical ophthalmology (Auckland, N.Z.), 13 (2019) 2553-2561.
[45] S. Rashid, Y. Jin, T. Ecoiffier, S. Barabino, D.A. Schaumberg, M.R. Dana, Topical Omega-3 and Omega-6 Fatty Acids for Treatment of Dry Eye, Archives of Ophthalmology, 126 (2008) 219-225.
[46] S. Pescina, L.G. Lucca, P. Govoni, C. Padula, E.D. Favero, L. Cantù, P. Santi, S. Nicoli, Ex Vivo Conjunctival Retention and Transconjunctival Transport of Poorly Soluble Drugs Using Polymeric Micelles, Pharmaceutics, 11 (2019) 476.

[47] S. Shubber, D. Vllasaliu, C. Rauch, F. Jordan, L. Illum, S. Stolnik, Mechanism of mucosal permeability enhancement of CriticalSorb® (Solutol® HS15) investigated in vitro in cell cultures, Pharmaceutical research, 32 (2015) 516-527.
[48] I. Pepić, J. Lovrić, J. Filipović-Grčić, How do polymeric micelles cross epithelial barriers?, European Journal of Pharmaceutical Sciences, 50 (2013) 42-55.
[49] M.S. Shahab, M. Rizwanullah, S. Sarim Imam, Formulation, optimization and evaluation of vitamin E TPGS emulsified dorzolamide solid lipid nanoparticles, Journal of Drug Delivery Science and Technology, 68 (2022) 103062.
[50] A. Labbé, C. Baudouin, D. Ismail, M. Amrane, J.S. Garrigue, A. Leonardi, F.C. Figueiredo, G. Van Setten, M. Labetoulle, Pan-European survey of the topical ocular use of cyclosporine A, Journal Français d'Ophtalmologie, 40 (2017) 187-195.
[51] E. Eljarrat-Binstock, J. Pe'er, A.J. Domb, New Techniques for Drug Delivery to the Posterior Eye Segment, Pharmaceutical Research, 27 (2010) 530-543.
[52] M.G. Traber, C.A. Thellman, M.J. Rindler, H.J. Kayden, Uptake of intact TPGS (d-alpha-tocopheryl polyethylene glycol 1000 succinate) a water-miscible form of vitamin E by human cells in vitro, The American Journal of Clinical Nutrition, 48 (1988) 605-611.
[53] S. Duvvuri, S. Majumdar, K.A. Mitra, Role of Metabolism in Ocular Drug Delivery, Current Drug Metabolism, 5 (2004) 507-515.
[54] E.M. Heikkinen, E.M. del Amo, V.-P. Ranta, A. Urtti, K.-S. Vellonen, M. Ruponen, Esterase activity in porcine and albino rabbit ocular tissues, European Journal of Pharmaceutical Sciences, 123 (2018) 106-110.
[55] P. Ichhpujani, L.J. Katz, G. Hollo, C.L. Shields, J.A. Shields, B. Marr, R. Eagle, H. Alvim, S.S. Wizov, A. Acheampong, J. Chen, L.A. Wheeler, Comparison of Human Ocular Distribution of Bimatoprost and Latanoprost, Journal of Ocular Pharmacology and Therapeutics, 28 (2011) 134-145.
[56] A.K. Grover, S.E. Samson, Antioxidants and vision health: facts and fiction, Molecular and Cellular Biochemistry, 388 (2014) 173-183.
[57] M.M. McCusker, K. Durrani, M.J. Payette, J. Suchecki, An eye on nutrition: The role of vitamins, essential fatty acids, and antioxidants in age-related macular degeneration, dry eye syndrome, and cataract, Clinics in Dermatology, 34 (2016) 276-285.
[58] B. Boldrini, E. Cavalli, A. Painelli, F. Terenziani, Polar Dyes in Solution: A Joint Experimental and Theoretical Study of Absorption and Emission Band Shapes, The Journal of Physical Chemistry A, 106 (2002) 6286-6294.
[59] F. Helmchen, W. Denk, Deep tissue two-photon microscopy, Nature Methods, 2 (2005) 932-940.
[60] C.Y. Park, J.K. Lee, R.S. Chuck, Second Harmonic Generation Imaging Analysis of Collagen Arrangement in Human Cornea, Investigative Ophthalmology & Visual Science, 56 (2015) 5622-5629.
[61] M. Zyablitskaya, E.L. Munteanu, T. Nagasaki, D.C. Paik, Second Harmonic Generation Signals in Rabbit Sclera As a Tool for Evaluation of Therapeutic Tissue Cross-linking (TXL) for Myopia, Journal of visualized experiments : JoVE, (2018) 56385.
[62] P.G. Watson, R.D. Young, Scleral structure, organisation and disease. A review, Experimental Eye Research, 78 (2004) 609-623.
[63] J.G. Hollyfield, M.E. Rayborn, M. Tammi, R. Tammi, Hyaluronan in the Interphotoreceptor Matrix of the Eye: Species Differences in Content, Distribution, Ligand Binding and degradation, Experimental Eye Research, 66 (1998) 241-248.
[64] J. Puig-Rigall, C. Fernández-Rubio, J. González-Benito, J.E. Houston, A. Radulescu, P. Nguewa, G. González-Gaitano, Structural characterization by scattering and spectroscopic methods and

biological evaluation of polymeric micelles of poloxamines and TPGS as nanocarriers for miltefosine delivery, International Journal of Pharmaceutics, 578 (2020) 119057.
[65] J.K. Pijanka, B. Coudrillier, K. Ziegler, T. Sorensen, K.M. Meek, T.D. Nguyen, H.A. Quigley, C. Boote, Quantitative Mapping of Collagen Fiber Orientation in Non-glaucoma and Glaucoma Posterior Human Sclerae, Investigative Ophthalmology & Visual Science, 53 (2012) 5258-5270.
[66] Y. Komai, T. Ushiki, The three-dimensional organization of collagen fibrils in the human cornea and sclera, Investigative Ophthalmology & Visual Science, 32 (1991) 2244-2258.
[67] K.M. Hämäläinen, K. Kananen, S. Auriola, K. Kontturi, A. Urtti, Characterization of paracellular and aqueous penetration routes in cornea, conjunctiva, and sclera, Investigative Ophthalmology & Visual Science, 38 (1997) 627-634.
[68] W. Chen, Z. Li, J. Hu, Z. Zhang, L. Chen, Y. Chen, Z. Liu, Corneal Alternations Induced by Topical Application of Benzalkonium Chloride in Rabbit, PLOS ONE, 6 (2011) e26103.
[69] E. Donnenfeld, S.C. Pflugfelder, Topical Ophthalmic Cyclosporine: Pharmacology and Clinical Uses, Survey of Ophthalmology, 54 (2009) 321-338.
[70] G.J. Jaffe, C.-S. Yang, X.-C. Wang, S.W. Cousins, R.P. Gallemore, P. Ashton, Intravitreal sustained-release cyclosporine in the treatment of experimental uveitis, Ophthalmology, 105 (1998) 46-56.